10-4-2010

The Virtual Hip: An Anatomically Accurate Finite Element Model Based on the Visible Human Dataset

Jonathan M. Ford
University of South Florida

The Virtual Hip: An Anatomically Accurate Finite Element Model Based on the Visible Human Dataset

by

Jonathan M. Ford

A thesis submitted in partial fulfillment
of the requirements for the degree of
Master of Science in Biomedical Engineering
Department of Chemical and Biomedical Engineering
College of Engineering
University of South Florida

Co-Major Professor: Don Hilbelink, Ph.D.
Co-Major Professor: Les Piegl, Ph.D.
William Lee III, Ph.D., P.E.
Karl Muffly, Ph.D.

Date of Approval:
October 4, 2010

Keywords: Quantitative Anatomy, Gluteus Minimus, COMSOL, Model Error

DEDICATION

I would like to dedicate this thesis to “B” and Vegas. They pushed me to reach for the stars and when I lost my direction they were the ones to point me the way.

ACKNOWLEDGMENTS

I would like to thank Dr. Don Hilbelink for his tireless efforts in mentoring me and providing me with the encouragement to keep pushing the limits. I thank Dr. Les Piegl for lending his computer expertise. I thank Dr. William Lee III for his constant support. I also thank Dr. Karl Muffly for being a voice of reason when I needed one. A special thanks goes out the College of Medicine and the Department of Pathology and Cell Biology for their funding support.

Thank you also to my parents for being my cheerleaders.

TABLE OF CONTENTS

LIST OF TABLES

LIST OF FIGURES

The Virtual Hip: An Anatomically Accurate Finite Element Model Based on the Visible Human Dataset

Jonathan M. Ford

ABSTRACT

The purpose of this study is to determine if element decimation of a 3-D anatomical model affects the results of Finite Element Analysis (FEA). FEA has been increasingly applied to the biological and medical sciences. In order for an anatomical model to successfully run in FEA, the 3-D model's complex geometry must be simplified, resulting in a loss of anatomical detail. The process of decimation reduces the number of elements within the structure and creates a simpler approximation of the model. Using the National Library of Medicine's Visible Human Male dataset, a virtual 3-D representation of several structures of the hip were produced. The initial highest resolution model was processed through several levels of decimation. Each of these representative anatomical models were run in COMSOL 3.5a to measure the degree of displacement. These results were compared against the original model to determine what level of error was introduced due to model simplification.

CHAPTER 1:

INTRODUCTION

Anatomy traditionally has been a descriptive science. Anatomical structures are named based on their shape, location and/or their relationship to the surrounding anatomical structures. Three-dimensional (3-D) anatomical features and relationships historically have been displayed in atlases composed of stylized drawings and more recently photographs. Advances in computer and medical imaging technology now permits the production of detailed 3-D models of anatomy for use as teaching and research tools. Research initiatives which began in the early 1990's with the Visible Human Project have now expanded to include data from different imaging modalities and have provided ever increasing insight into how the human body is organized.[1]

Utilizing tools from other fields such as engineering, anatomists have begun to create anatomically accurate 3-D models for use in medical education and research. One such tool, the Finite Element Method (FEM), utilizes two-dimensional (2-D) and 3-D geometry to gain a better understanding of how an object physically functions. Finite Element Analysis (FEA) can be used as a precursory step to predict the outcome of a physical event before actually

running an experiment or manufacturing an expensive prototype. Applying FEM to the study of human anatomy permits detailed analysis of complex virtual anatomical models under simulated experimental conditions.[2]

Despite the current level of today's advanced computer technology, there are still limitations to applying FEA for biological models. The complex geometries and the subtle details of anatomical structures can prove too intricate for FEA to work. As a result, 3-D models must often be decimated to such an extent that a significant reduction in anatomical detail may result. The trade off is a more simplified approximation of the original object that is no longer anatomically accurate and may affect the FEA results.

The question remains as to how much decimation is acceptable. The answer depends on a variety of factors such as the goals of the research project, the functional importance of certain features, and the hardware and software capabilities. The purpose of this study is to determine if element decimation of a 3-D anatomical model affects the results of FEA.

In this study two versions of a high-resolution 3-D model of the human hip from the Visible Human Male dataset were developed. One model contained the actual geometry of the gluteus minimus and the other model contained a cylindrical arm representing the same muscle. A test simulation was run in COMSOL comparing the displacement of the distal end of the femur. The results

of each simulation were compared against the model's complexity. For the purposes of this study, complexity was represented by the decrease in the number of elements in the gluteus minimus model. These findings were used as an example of the possible effects of model simplification.

By creating a virtual 3-D hip and decimating the geometric meshes that make up the gluteus minimus, the results of this study will inform anatomists, clinicians, and biomedical engineers what affects the loss of anatomical detail has in a model's behavior and also flag what features should be preserved.

CHAPTER 2:

BACKGROUND

Anatomy

Early anatomists like Galen, based their anatomical knowledge on observations made from dissecting wild and domestic animals. The birth of modern human anatomy is credited to a Belgian medical student named Andreas Vesalius (1514-1564).[3] His work, *On the structure of the Human Body*, inspired generations of anatomical scholars. Taking their cue from Vesalius, the use of illustrated textbooks in conjunction with cadaver dissection became standard tools in medical education. Netter's *Atlas of Human Anatomy*, *Grant's Atlas of Anatomy* and the current version of *Gray's Anatomy* are common resources in modern medical schools across the United States. All these atlases are static 2-D representations of 3-D anatomical structures. [4]

Visible Human Project

The National Library of Medicine's Visible Human Project was initiated in 1989 with the goal to create a digital volumetric collection of complete normal adult male and female anatomy. The Visual Human Male (VHM) dataset was

completed in August of 1993. The specimen was that of a 39-year-old male incarcerated on death row in the Texas prison system and who had donated his body to science. His donation began a nine-month process of imaging, freezing and sectioning the specimen for the creation of the dataset. The specimen remained frozen in a gelatin block for 46 days at a temperature of -7º C or below. Due to the size limitations of the custom cryomacrotome developed by the University of Colorado, the specimen was sectioned into four blocks with dimensions no larger than 22 inches in height, 21 inches in width and 14 inches in depth. Over a period of 128 days the specimen was milled in 1 mm increments using the cryomacrotome. A series of film and digital photographs were taken for each slice through the specimen.

The VHM dataset consists of the initial MRI and CT scans and the digital collection of color images. This digital information is roughly 15 gigabytes in size. The 1,878 axial images are tiff files that are 1760 x 1024 pixels in size with a resolution of 72 dpi and in total take up roughly 9.5 gigabytes of space. The dataset is public domain and available from the National Library of Medicine (NLM).[6] Following release of the Visible Human Male, a number of similar projects were undertaken. In the years that followed, the NLM released the Visible Human Female. Other groups released their own versions such as the Visible Korean Project[7] and the Visible Chinese Project[8].

What makes the visible human datasets unique is the ability to observe the anatomy of an entire individual in situ. The spacing of organs and structures remain in their natural location as they were in a living body. The availability of these high-resolution images provides for the first time the opportunity for the accurate reconstruction of the human body. Three-dimensional and four-dimensional representations of human anatomy are now possible as a result of advances in high-resolution medical imaging modalities such as Magnetic Resonance Imaging (MRI) and Computed Tomography (CT). High-resolution anatomically accurate 3-D models can now be visualized and manipulated using readily available software and analyzed and measured using application based software for Computer-Aided Design (CAD) and Finite Element Analysis (FEA).

Finite Element Analysis

FEA or the Finite Element Method (FEM) has become standard practice in the development of models and simulations for a variety of engineering projects. The term was first coined by R.W.Clough in 1960 with his discussion concerning plane stress analysis.[9] The lessons learned from the early applications of FEA were quickly adopted and utilized the fields of thermal, fluid flow and piezoelectric process. FEM is now used in transportation, electrical, communications, housing, environmental, acoustical, as well as biological and medical applications. The ability to model, visualize, analyze, simulate, prototype and fabricate structures

has opened up the possibilities and the usefulness of computers in the engineering process.[10,11]

The main goal of FEM is to determine the distribution of a property throughout the structure based on a set of partial differential equations. A few common examples of these potential properties can be temperature disbursement, the displacement from an applied stress, or the distribution of an electrical charge. At the beginning of this process, the engineer calculates the acting agent for each element of the structure. This agent can take the form of force, electrical current, temperature and so on. The result is an approximated solution that numerically represents the distribution of a problem that would be considerably difficult to obtain manually. FEM can be applied to one-dimensional, two-dimensional, three-dimensional and four-dimensional problems. The model is sectioned into a number of simplistic geometric elements. These elements range from tetrahedral (four-sided), brick (8-sided) to hexahedral (6-sided) in shape. The number of elements is finite and in turn each element has a set of known physical laws and finite parameters applied to it. The process creates a set of linear algebraic equations that are run simultaneously to solve the system.[11]

The real objects and their relative components can be rather complex and often need to be decimated so that the finite element software package can handle the geometry. The structure's geometry is created from the collection of elements that provide a discretized approximation of the object's curves in a piecewise

fashion. This occurs via a process known as meshing. The accuracy of the curve's representation hinges on the number of elements that are used in the mesh. It follows that the closest representation of a structure would have the highest number of elements. However, each element requires its own computation. Due to software and hardware limitations, it is essential to cap the number of elements used. On account of these limitations, the finer details of a structure are often omitted. It is up to the designer or modeler to determine whether or not the smaller details are critical to the overall structure. If these details play only an aesthetic or minimal role in the performance then their exclusion is considered acceptable. A greater quantity of elements in the mesh corresponds to a closer representation of the actual geometry. The results of the analysis need to be observed with these omissions firmly in mind. In the end, all finite element analysis results in the approximation of the structure or structures being studied. It may be a very close approximation, but it is still an approximation nonetheless. [11]

The creation of a mesh can be an arduous process. The length of time needed in mesh creation lies in the object's complexity and the experience of the analyst. Meshing via triangulation is the most common form of element creation. Unlike brick meshes, the creation of tetrahedral meshes is highly automated in most pre-processing software. Tetrahedral meshes also have the added advantage of being able to tackle complex organic geometries. However, the speed and ease

of tetrahedral meshes comes at the cost of accuracy. Brick element meshes are considered more accurate, but their lack of automation decreases their use.[11]

Once the mesh is created the object is assigned material properties. Objects can be made up of multiple materials based on the Young's modulus and shear modules of the desired material. These properties can be assigned to a group of elements or to each individual element. Commercially available FEM packages often come with a built-in library of known material values. These usually consist of different types of metals and other materials such as wood or glass. Most packages do not come with biological materials and the properties for these items need to be furnished from experimental data. A number of publications exist that have suggested material properties for objects of a biological origin, such as bone or soft tissue. The Poisson's ratio and density of the material is often lacking.[12-17] The solving of the computational model utilizes a computer's Central Processing Unit (CPU) and the Random Access Memory (RAM). Obviously, the functionality of a computer improves as its processor and memory power increases.

There are a number of Finite Element software packages available for commercial use. A few of note include COMSOL, ANSYS and Abaqus. Each package is designed to accept a variety of file formats. Templates for common applications, such as electrical, thermal, acoustical, structural, fluids scenarios, are usually provided. All of these packages allow for user customization so the

analyst has full control of their model and simulation. As multi-physics packages, it is possible to include more than one physics interaction. For example, a finite element analysis can be run on a circuit for multiple scenarios. One analysis can compute the flow of electricity, while another determines the heat that corresponds with the generated electric current. Structure geometry can be created using native creation tools or imported from another software package.

Biological Applications

Finite Element Analysis chiefly has been used by engineers as a step in the manufacturing of products. More recently researchers from the biological sciences have tapped into finite element analysis to study the mechanics of organisms. The subjects studied are almost as varied as the number of organisms that exist past and present. Simulations have been made for insect flight,[18] feeding mechanics of animals,[19,20] defensive performance of extinct animals,[21] and plant biomechanics[22] to name a few. It must be stressed that the forces at work in these types of experiments are often hypothetical. For example, an FEA concerning the bite force of an animal must have the muscle forces and bones available from in vivo experimental data. The results of this experiment would be theoretical without physical testing. In cases where a study is being done concerning an extinct species, in vivo data would be impossible to acquire and the ultimate solution from an accompanying FEA analysis would be un-testable. Added difficulty exists in the modeling of biological geometries. Unlike

standard, predefined shapes and curves used in other engineering practices, biologically derived geometries must be either modeled by hand, a time consuming and potentially inaccurate process, or captured through one of the many scanning modalities.[25]

Human Applications

In addition to biological applications, FEA has been applied to humans and has assisted in a variety of medical and design fields. The mechanical behavior of the femur using a 2-D model was analyzed as early as 1972.[24] Blood flow[25], arterial wall pressure[26], foot tread analysis[27] and a number of other medically applicable studies have utilized the tools of the finite element method. Medical implant design and performance have also benefitted from finite element simulations.[28] Furthermore, the FE method has been applied to human models for design purposed in the automobile industry. One such example involves the creation of a model of the human body for restraint system testing applications.[29]

The field of Orthopedics has greatly benefited from the FE method. One example of finite element analysis used in a medical application can be seen in Helwig's study on the performance of a proximal femur nail. In this study femur data was captured using CT scanning. A force was applied to the femur to simulate a patient standing on one leg. Muscle tension was not considered. The femur model retained its hollow medullary cavity which was filled by a model of the

femoral implant. Two factures were modeled to represent the damaged bone. Under their analysis the femoral implant failed with the dislocation of the axial head screw. They credited this to the tilting of the proximal bone fragment. The researchers compared their results to clinical observations and determined that their model provided some clues to the implants performance, but that it was limited in its exclusion of musculature and the assumptions made on the isotopic material behavior of cancellous bone. They concluded that their results provided hints to explain some of the clinical observations but suggested an improved model would be better suited to answer those questions. Improvements in the modeling of muscles and their ultimate inclusion in more complex models are the focus of other studies.[30]

Much of FEA focuses on how muscles are modeled and their functions. Many computer models focusing on the musculoskeletal system represent muscles as line segments.[31-33] Software, such as Software for Interactive Musculoskeletal Modeling (SIMM)[34] and LifeModeler[35], have been developed to simulate the biomechanics of movement in both humans and animals. These software packages often utilize moment arms to control the model's movement.[36] There have been attempts to model the complex 3-D muscular geometry by focusing on the fibers that make up the muscles themselves. Some studies focus on the perpendicular arraignment of muscle fibers to try and capture shear stress and analyze stretch distributions during muscle exertion.[37] Still others try capture the 3-D arrangement and lengths of the muscle fibers to capture muscle behavior.[38]

These studies all focus on the 3-D geometry of the muscle to varying degrees of complexity.

Muscle Anatomy

The focus of this study was to examine the effect model simplification has on the biomechanics of the gluteus minimus and its associated osseous structures. The gluteus minimus lies beneath the gluteus medius and is a fan-shaped muscle whose origin is the upper portion of the ileum and inserts into the anterolateral face of the greater trochanter of the femur. The gluteus minimus is innervated by the superior gluteal nerve. This muscle abducts the lower limb at the hip and also stabilized the head of the femur in the acetabulum during walking or running.[39, 40] Dysfunction of the gluteus minimus often is associated with that of the gluteus medius due to their shared nerve supply and may result in Trendelenburg gait. The disorder causes the pelvis to sag on the non-affected side during a single leg stance on the affected side. Individuals with Trendelenburg gait compensate for their muscle weakness by leaning the torso toward the damaged side when their weight is on the affected limb.[41]

A finite element model involving the gluteus minimus, the femur and innominate (os coxa) bone and the ligamentum teres, was created to test the importance of anatomical geometry. The anatomy was based on the VHM dataset. For Phase 1, the gluteus minimus was decimated in a stepwise fashion. For each iteration, a

finite element analysis of displacement was conducted and the results were compared to determine what impact geometric simplification had on the models performance. For Phase 2, the geometry of the gluteus minimus was replaced with a moment arm to test the influence of the muscle's origin and insertion.

CHAPTER 3:

MATERIALS AND METHODS

Dataset

The National Library of Medicine's (NLM) Visible Human Male dataset from the Visible Human Project was used as the initial source for the development of anatomically accurate models. The entire dataset is available for download upon request from the NLM's website.[43] In total, the dataset consists of 1,878 slices as a tagged image file format (tiff) each with a resolution of 1760 x 1024. Each slice is 1 millimeter thick with a pixel size of 0.3528 millimeters. The slices are numbered in a fashion ranging from 1,001 to 2,878. Each color image was then hand segmented using Adobe's *Photoshop*. Every structure segmented was assigned its own red, green and blue (RGB) value. This was a lengthy process that took a number of trained hands a considerable amount of time. An example of an original image and a segmented image can be seen in Figures 3.1 and 3.2 respectively.

Figure 3.1 Example of original image. This is slice 1870 of the Visible Human Male.

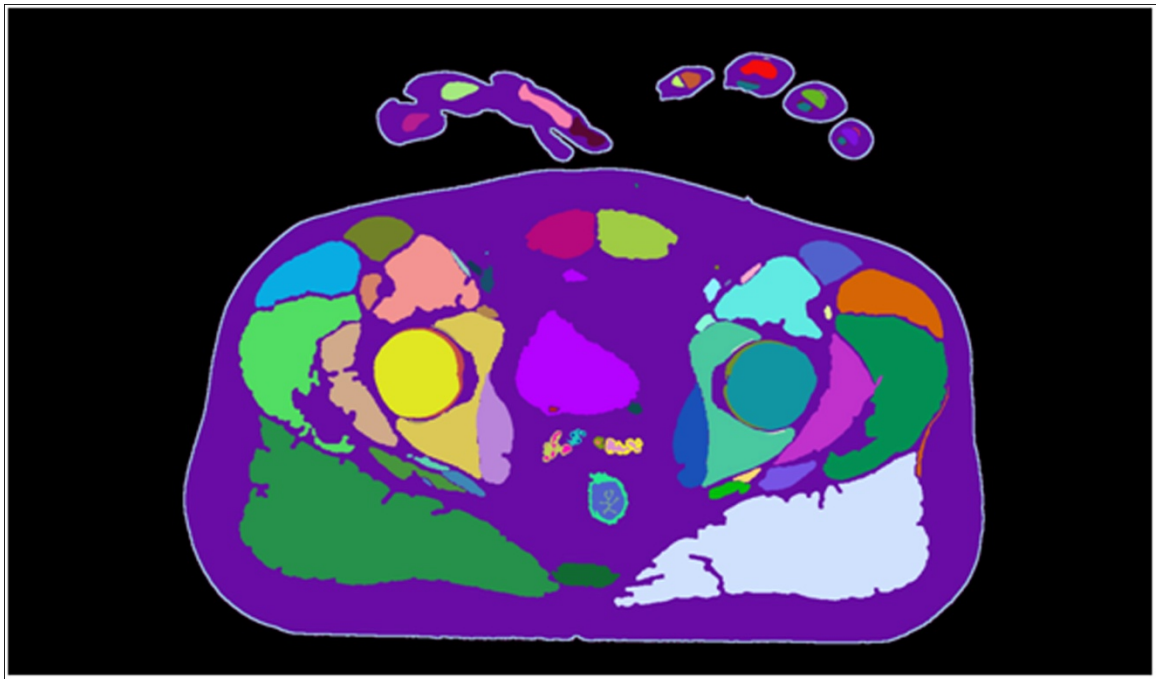

Figure 3.2 Example of segmented image. This is slice 1870 of the Visible Human Male. Courtesy of Dr. Don R. Hilbelink.

Making the Models

For the purposes of this study, all model creation was performed on a workstation with a 64-bit version of Windows 7 Professional. The computer had 48 gigabytes of RAM and an Intel Xeon X5677 3.57 gigahertz computer processing unit. The video card was an NVIDIA Quadro FX 5800. This computer will be referred to as desktop for the remainder of the paper.

The structures of interest in the scope of this study was limited to the VHM's left os coxa and femur bone as well as the left gluteus minimus muscle. An artificial ligament representing the ligamentum teres was created to anchor the femoral head to the acetabulum. The initial modeling steps occurred in the *Mimics 14.0* software package by Materialise. Due to the size of the segmentation data (9.45 gigabytes), only the slices relevant to the anatomy of interested were imported into *Mimics*. This included slices 1725 through 2350 for a total of 625 slices.

Upon import into *Mimics*, the RBG values were automatically converted to a 12-bit gray value with a scale of 0 to 4095. Once imported, the structure was assigned its own mask which was limited to the exact gray value allowing for the exclusion of all other structures. A three-dimensional (3-D) model of the structure was created using the optimal preset setting once the mask creation was complete. *Mimics* uses a triangular tessellation method to create 3-D geometries.

An example of the *Mimics* user interface displaying the conversion to grayscale, mask editing and the rough 3-D geometry can be seen in Figure 3.3.

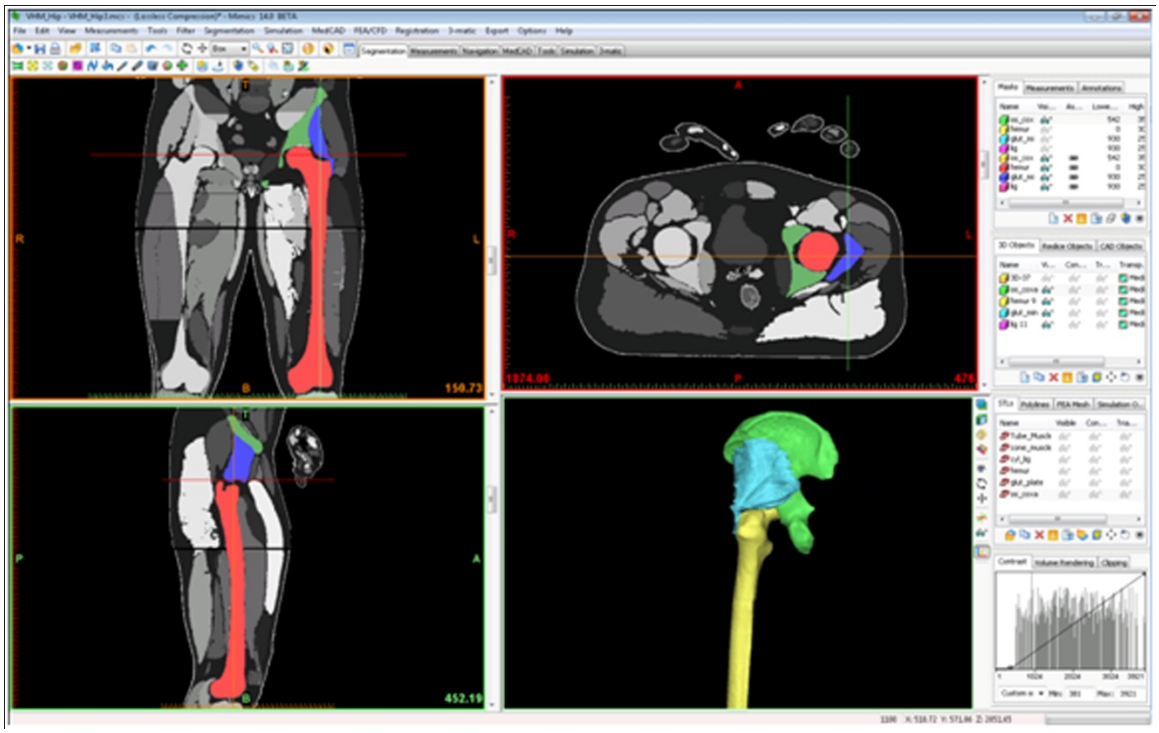

Figure 3.3 Example of Mimics 14.0 user interface.

Due to the size limitations of the milling devices used in the sectioning of the visible human male, the specimen was cut into four blocks. The division of the specimen into the four blocks left the Visible Human Male with three sections of missing data. To account for the missing slices and the volume they would have occupied, blank sections were left in their place. During model creation, this lost data was recreated using the interpolation features of Mimics. The only anatomical structure used in this study that was affected by this procedure was the left femur.

Once the initial step of the modeling was complete, each model was exported as a binary stereolithographic file (stl). The stl for each structure was then imported into *3-Matic 5.1*, also by Materialise, for analysis, quality control and remeshing. In this program the 3-D anatomy was cleaned up and converted to a volumetric mesh. The initial model clean up began with a wrapping procedure to ensure each model was one solid object. This step was followed by a Triangle Reduction filter which had a flip threshold angle of 15˚ and a geometrical error of 0.05 mm. Model cleanup continued by applying a smoothing factor of 0.7 to the object. Once these steps were complete, the model was then inspected for any intersecting or overlapping triangles. Any errors were quickly fixed before moving onto the creation of a volumetric mesh. To create a volume mesh the structures were combined using the “Create Non-Manifold” mesh option. Surfaces on the mesh were assigned at this step to ensure at a standardized shape and location was maintained through the process.

For Phase 1, the model underwent a series of processing steps involving: autoremeshing and quality reduction of triangles of the gluteus minimus. The overall model was inspected for intersecting or overlapping triangles and finally, converted to a volumetric mesh. The simplification of the gluteus minimus took place in the autoremeshing and quality reduce triangles procedures. The level of mesh complexity was reduced by increasing the maximum geometric error allowed. Nine levels of model complexity were created in this manner. The most complex model allowed for a maximum geometric error of 0.01 mm. The model

decreased in complexity as the maximum geometric error was increased in a stepwise fashion. The levels of geometric error were included in this study were 0.01 mm, 0.04 mm, 0.05 mm, 0.1 mm, 0.11 mm, 0.15 mm, 0.25 mm, 0.75 mm, and 1 mm. Intermediate steps were made, but the resulting percentage of reduction were not dramatically different. The 1 mm geometric error was chosen as the stopping point for model simplification as it resulted with a 90% reduction in the number of elements. After the finial simplification step was completed, the models were then converted into volume meshes of tetrahedral elements. The surface and volume meshes were then exported as MPHTXT files, the *COMSOL* ready mesh format. The resulting models consist of a non-manifold mesh of the left innominate bone, left femur, ligamentum teres and the left gluteus minimus at different levels of simplification.

Phase 2 of this study examined the importance of the muscle geometry as compared to the interaction with the origin and insertion. For this model the bones and the ligamentum teres remained unchanged. The gluteus minimus was removed and a curved cylinder stretching from the center of the muscle's origin and insertion was created in its place to represent the muscles line of action. The surface of the origin and insertion of the original gluteus minimus geometry was left in place.

COMSOL

Each decimated iteration of the gluteus minimus mesh was imported into *COMSOL 3.5a* and run on an individual basis under the 3-D structural mechanics module native to the program. The material properties were the same for every model. The bones were given a Young's modulus of 1.0×10^{10} Pa, a Poisson's ratio of 0.3 and a density of 2570 kg/m.[43] The gluteus minimus was given a Young's modulus of 1.162×10^{6} Pa, a Poisson's ratio of 0.4 and a density of 1200 kg/m^3.[44] The ligamentum teres was given a Young's modulus of 3.66×10^{8} Pa, a Poisson's ratio of 0.40 and a density of 1200 kg/m^3.[44] The Poisson's ratio and density for ligament tissue were not available so the respective values were filled with the equivalent for muscle tissue. The pubic sympheseal surface was constrained in the X, Y and Z directions to lock the pelvis in place. A point central to the distal end of the femur was selected and used as the b asis for each measurement comparisons.

For the first phase, a force of -5.0×10^{5} N/m^2 was applied to the interface between the gluteus minimus and the os coxa in the X direction and a force of 5.0×10^{5} N/m^2 was applied in the Z direction. No force was applied in the Y direction. The model was then solved to determine the amount of displacement that occurred at the designated point of measurement.

For Phase 2, the model containing the representative arm of the gluteus minimus was run under two different scenarios. Scenario 1 utilized the surface area representing the origin of the gluteus minimus and received the same amount of force as Model 1. Scenario 2 utilized only the surface areas where the arm or arms made contact with the innominate bone. The amount of force needed to be adjusted proportionally to the surface area of the interface between the arm. The proportionally adjusted applied force was of -5.61×10^7 N/m^2 in the X direction and 5.61×10^7 N/m^2 in the Z direction.

The level of displacement was collected in the individual X, Y and Z directions as well as the total displacement. It was assumed that the highest level of complexity for the first phase was the closest approximation to the actual geometry. The results for this model were used as a baseline for comparison. The percentage of simplification (based on the decreased in the number of elements) and the percentage of error from this baseline model were calculated for each decimated version of the gluteus minimus as well as the models for Phase 2.

CHAPTER 4:

RESULTS

Models

In Phase 1, nine FE models of the human hip containing the left femur, innominate bone, and a representation of the gluteus minimus and ligamentum teres were created from the VHM. The number of elements in the gluteus minimus were reduced systematically. The model with the highest level of complexity consisted of a total of 468,813 tetrahedral elements with the gluteus minimus consisting of 65,960 elements. This model was used as the baseline for all model comparisons. The number of elements in the gluteus minimus were reduced to 6,995 at its highest level of decimation. The model demographics and displacement data can be found in Appendix A.

The gluteus minimus in Phase 2 was replaced with a curved cylinder representing the central most path of the muscle. This model consisted of 411,464 elements with the represented gluteus minimus consisting of 5,832 elements. A table showing the number of elements for each iteration of the Phase 1 models and the percentage of element reduction can be seen in Table

4.1. A visual representation of the models for Phase 1 and Phase 2 can be seen in Figure 4.1.

Table 4.1 Number of elements and percentage reduction for each level of model simplification

Total Elements	Total Reduction	Gluteus Minimus Elements	Gluteus Minimus Reduction
468,813	0%	65,960	0%
457,258	2%	56,933	14%
449,382	4%	51,903	21%
445,351	5%	43,946	33%
423,665	10%	32,370	51%
414,914	11%	26,040	61%
402,416	14%	17,299	74%
388,337	17%	8,049	88%
387,148	17%	6,995	89%

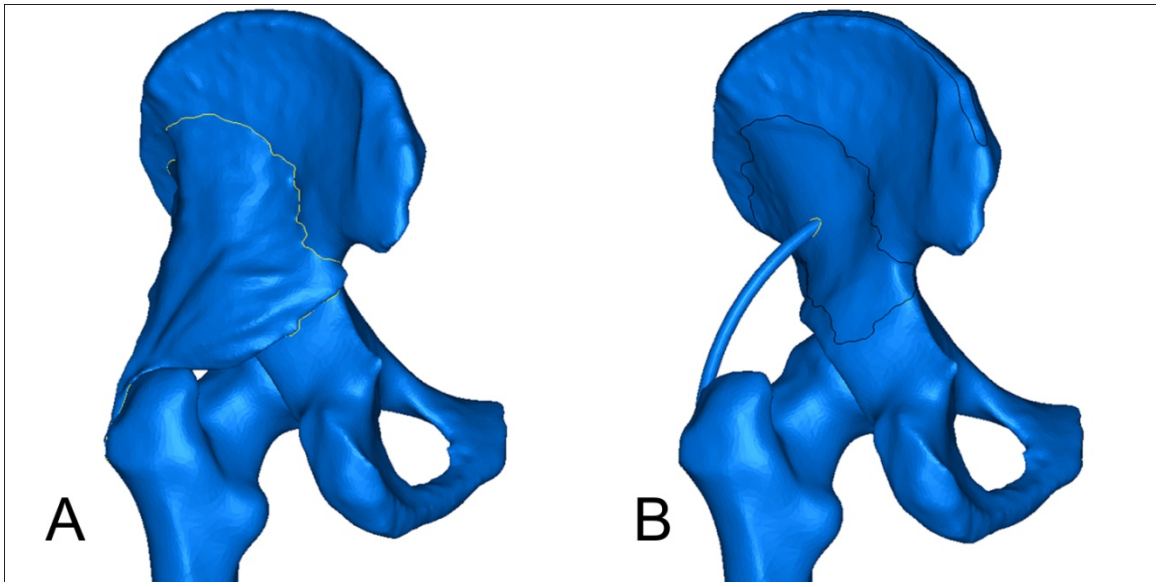

Figure 4.1 Image of Phase 1 model (A) and image of Phase 2 model (B).

COMSOL

A structure analysis for the degree of displacement was run in COMSOL 3.5a of each model for Phase 1 and Phase 2. Figure 4.2 contains a representative visual plot of the displacement using the most complex model of Phase 1.

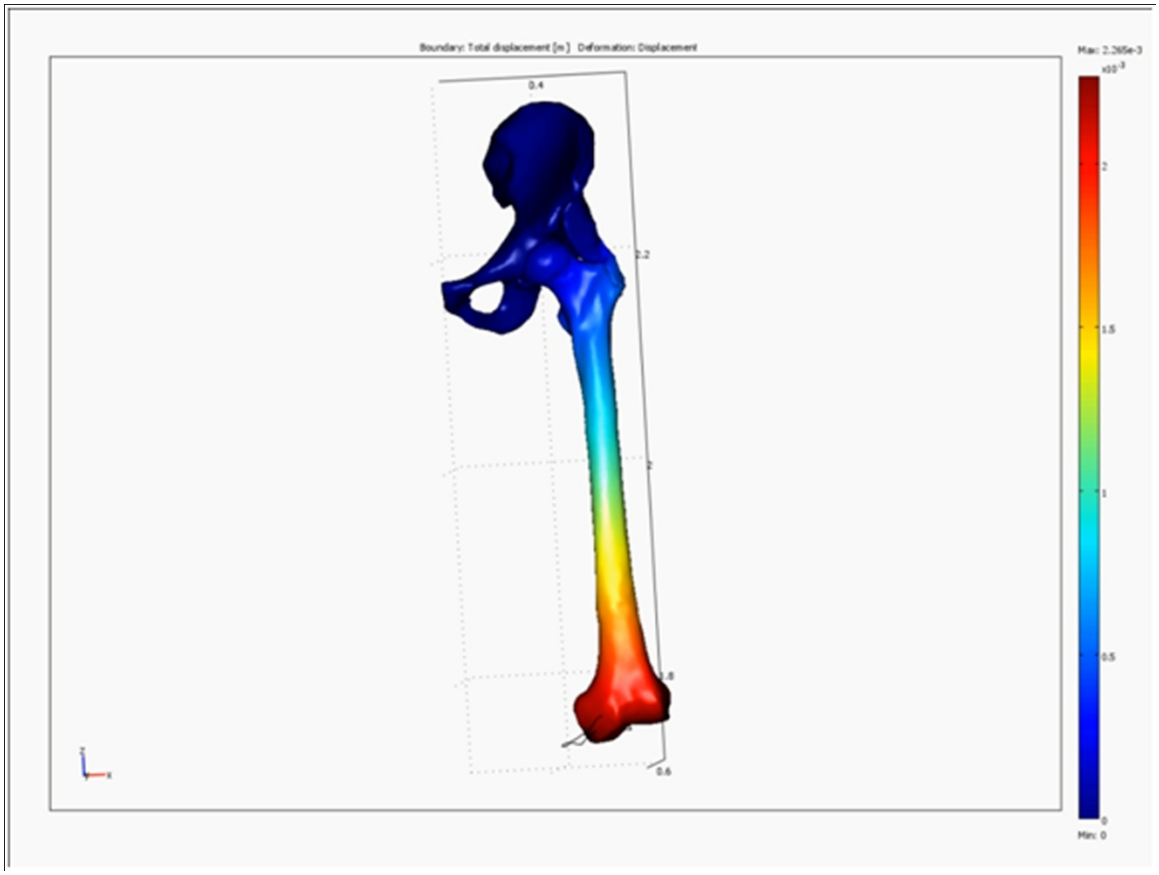

Figure 4.2 Displacement plot of the most complex model of Phase 1.

Displacement

The overall displacement of the distal end of the femur was calculated for each model. The gluteus minimus model with the highest number of elements was used as a baseline for comparison in calculating the percentage of element reduction and percentage of error in displacement. Table 4.2 shows the breakdown of the percentage of element reduction, the distances for the direction and total movement, the percentage error of displacement and the solution speed for each level of simplification for Phase 1. Figure 4.3 shows a plot comparing the element reduction percentage versus the total displacement error as well as the individual X, Y and Z directions. Figure 4.4 provides a plot of the actual displacement in millimeters for each iteration of simplification in Phase 1.

Table 4.2 Displacement for Phase 1

Percent of Reduction	X Movement	Y Movement	Z Movement	Total Movement	X Error	Y Error	Z Error	Total Error	Solution Time
0.00%	155.19	44.91	39.46	166.31	0.00%	0.00%	0.00%	0.00%	1121
2.86%	155.14	44.88	39.44	166.25	0.03%	0.07%	0.05%	0.04%	896
3.63%	155.15	44.86	39.44	166.26	0.03%	0.11%	0.05%	0.03%	942
0.15%	155.17	44.87	39.45	166.27	0.01%	0.09%	0.03%	0.02%	904
2.54%	155.17	44.92	39.45	166.29	0.01%	0.02%	0.03%	0.01%	689
3.80%	155.19	44.91	39.46	166.31	0.00%	0.00%	0.00%	0.00%	641
7.91%	155.2	44.9	39.46	166.32	0.01%	0.02%	0.00%	0.01%	600
8.59%	155.2	44.92	39.46	166.32	0.01%	0.02%	0.00%	0.01%	576
11.56%	155.22	44.93	39.47	166.34	0.02%	0.04%	0.03%	0.02%	539

a) All movement in mm.

b) Solution time in seconds.

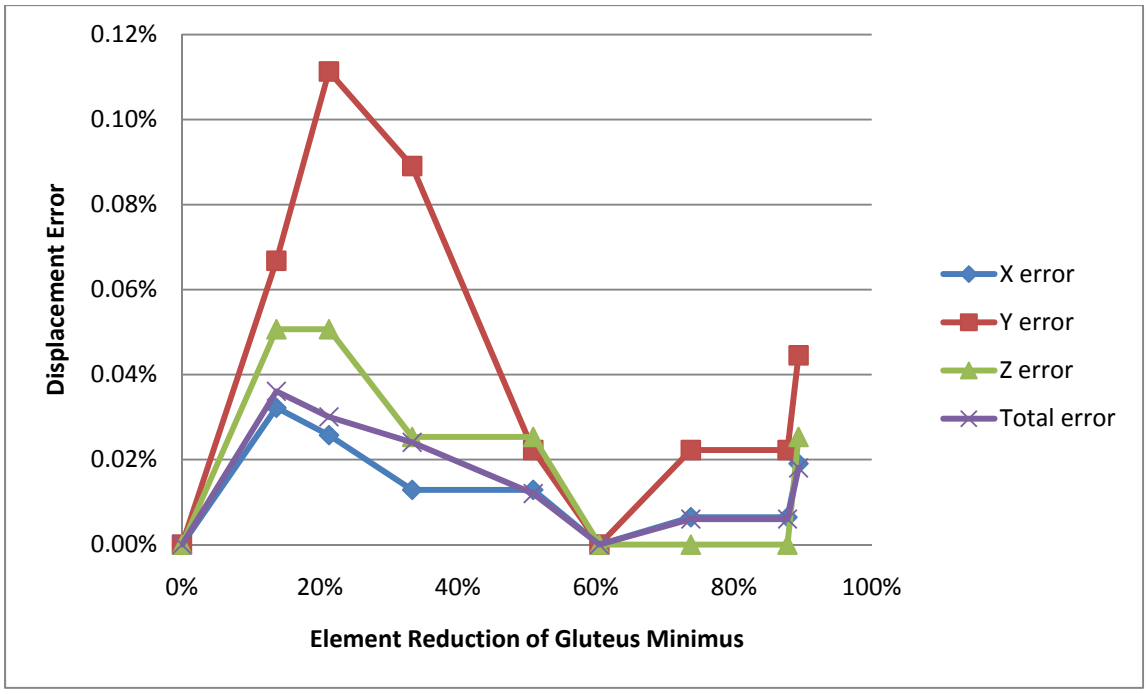

Figure 4.3 Plot of element reduction versus displacement error.

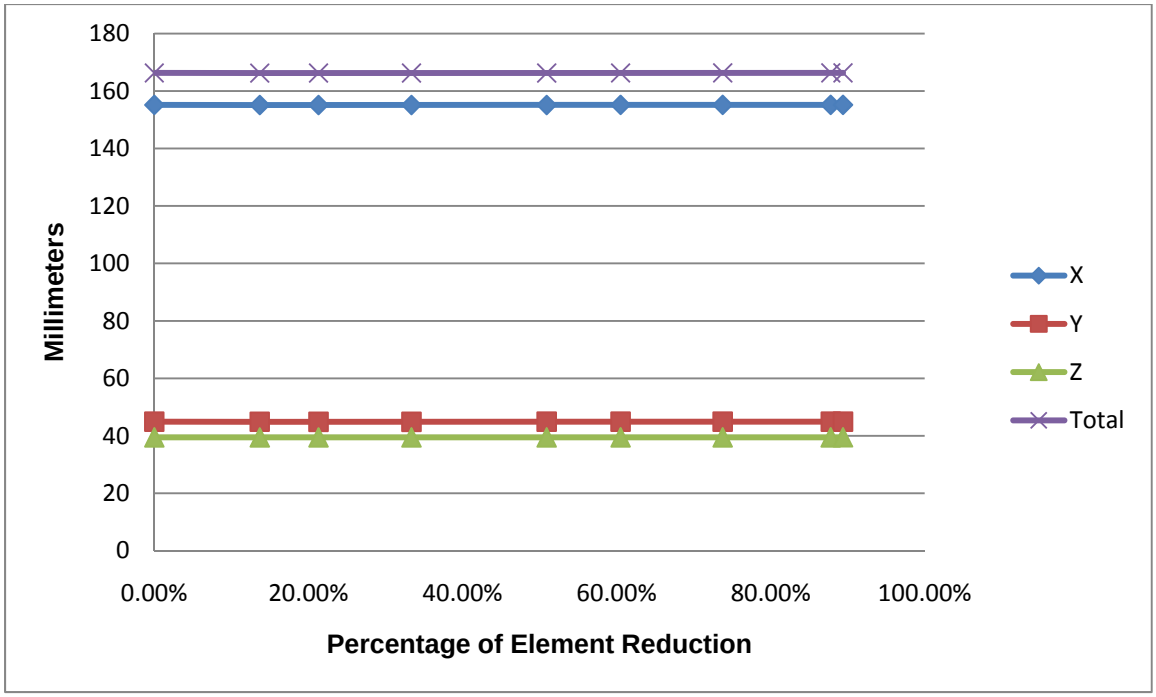

Figure 4.4 Plot of displacement in millimeters for Phase 1.

For Phase 2, the displacement of the distal end of the femur using the gluteus minimus muscle was compared against the single-arm model. The degree of displacement was determined with and without using the origin and insertion for the gluteus minimus. The gluteus minimus muscle with the highest number of elements was used as a baseline for comparison in calculating the percentage of element reduction and percentage of error in displacement. Figure 4.5 shows a plot comparing the displacement with and without using the geometry of the gluteus minimus' origin and insertion. Table 4.3 shows the breakdown of the distances for the direction and total movement, the percentage error of displacement and the solution speed for Phase 2.

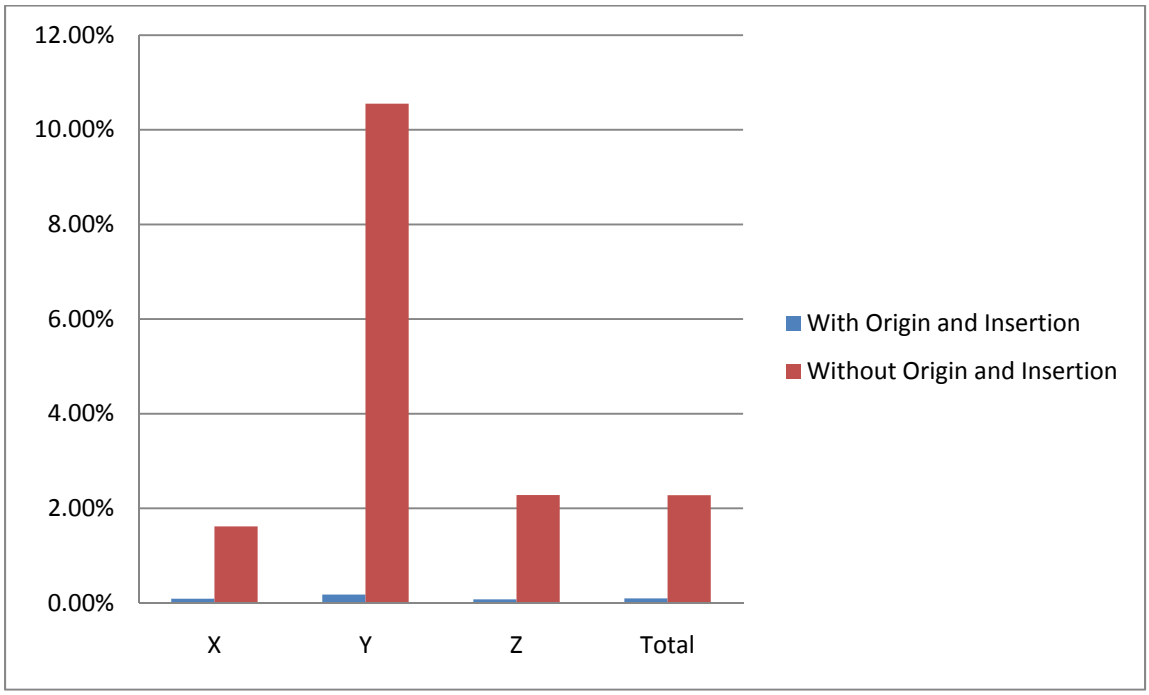

Figure 4.5 Plot of displacement with and without utilizing the origin and insertion.

Table 4.3 Displacement for Phase 2

Iteration	X Movement	Y Movement	Z Movement	Total Movement	X Error	Y Error	Z Error	Total Error	Solution Time
Original	155.19	44.91	39.46	166.31	0%	0%	0%	0%	1121
With Origin	155.05	44.83	39.43	166.15	0.09%	0.18%	0.08%	0.10%	660
Without Origin	152.68	40.17	38.56	162.52	1.62%	10.55%	2.28%	2.28%	664

a) All movement in mm.

b) Solution time in seconds.

Visual Comparison of Simplified Models

The alteration to the model's geometry as the mesh is simplified can be appreciated visually as well. Visual representation comparing the high resolution hip to the middle resolution hip and a low resolution hip can be seen in Figures 4.6, 4.7, and 4.8 respectively.

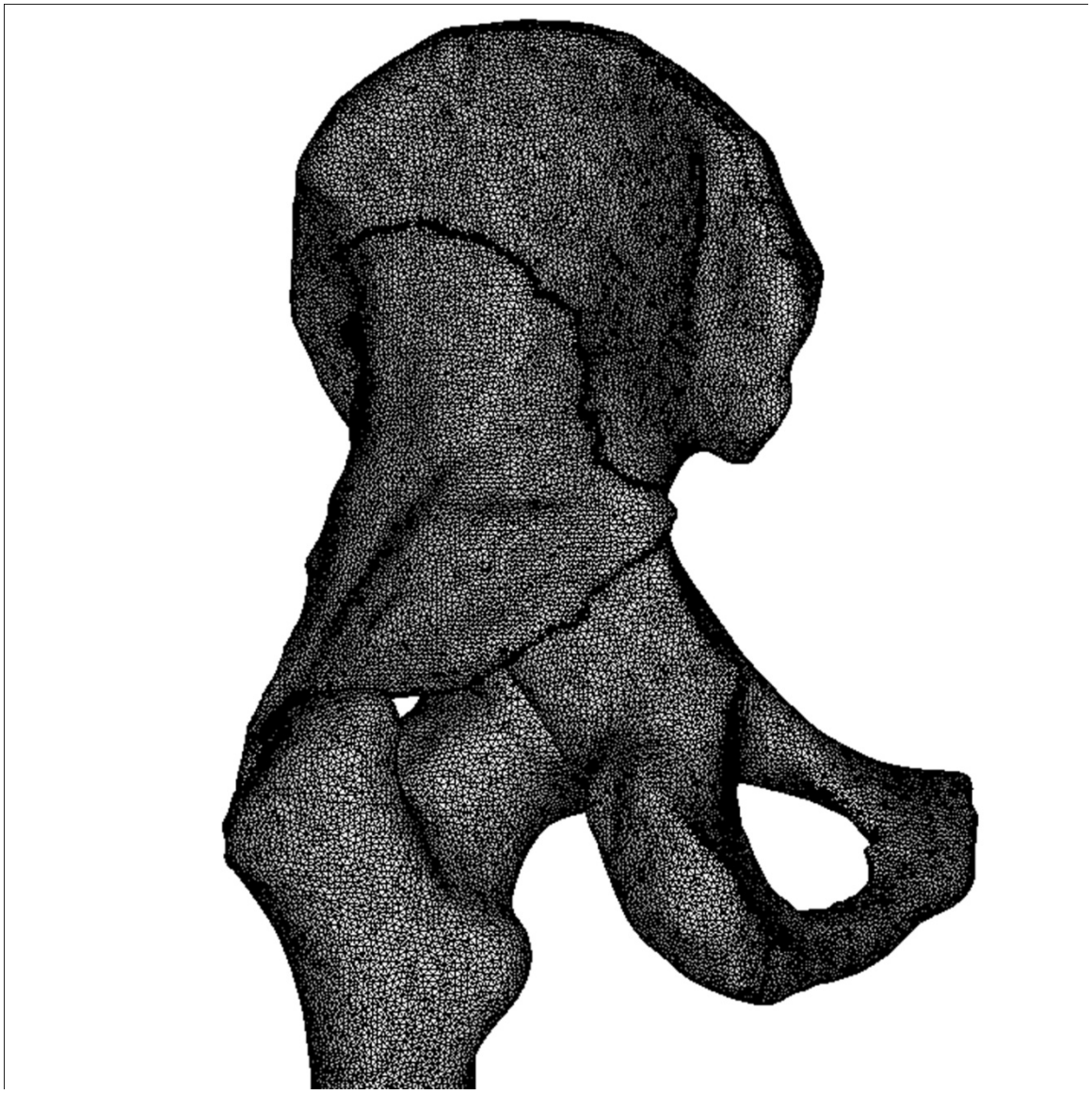

Figure 4.6 High-resolution gluteus minimus model consisting of 65,960 elements.

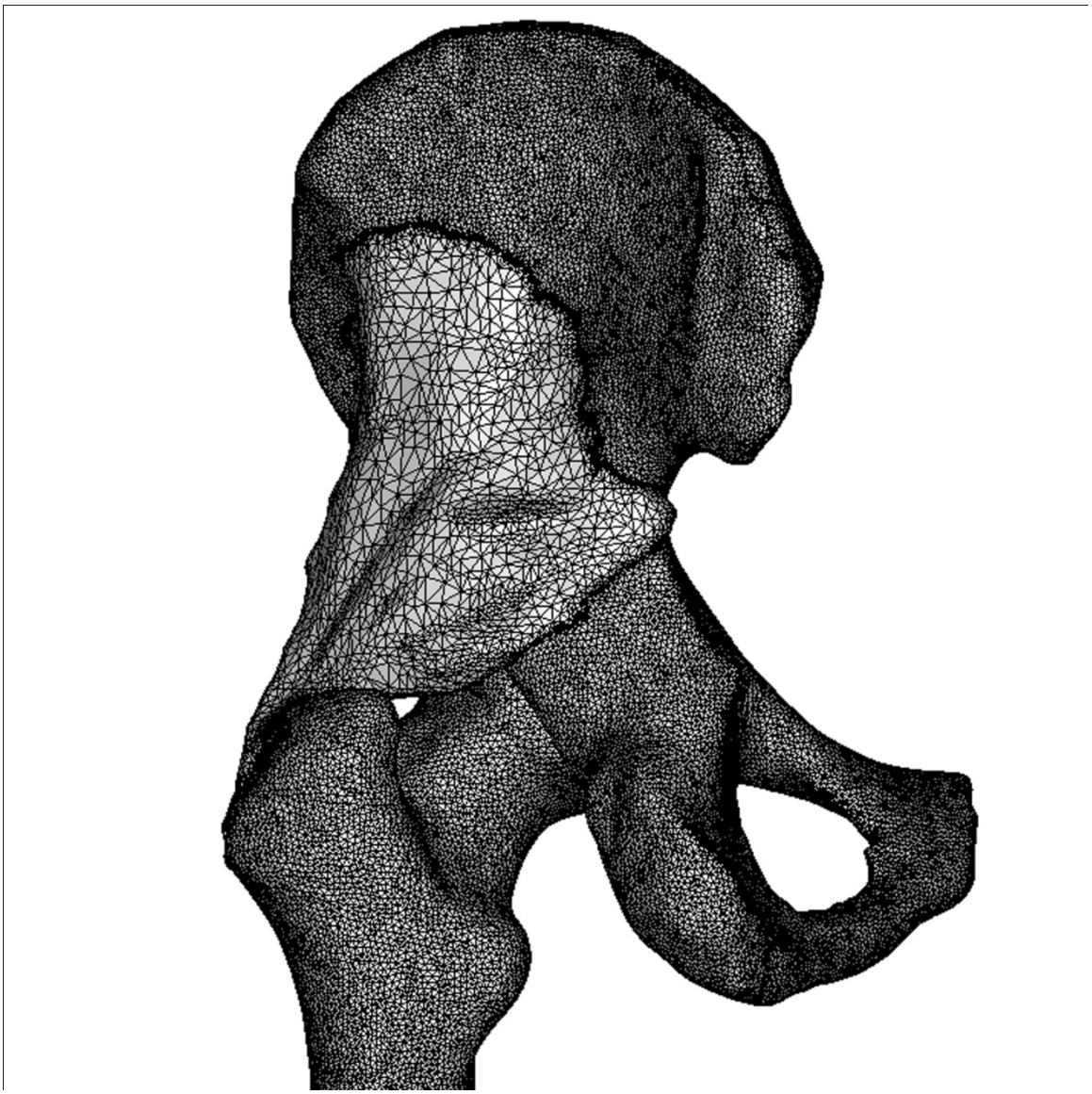

Figure 4.7 Mid-resolution gluteus minimus model consisting of 26,040 elements.

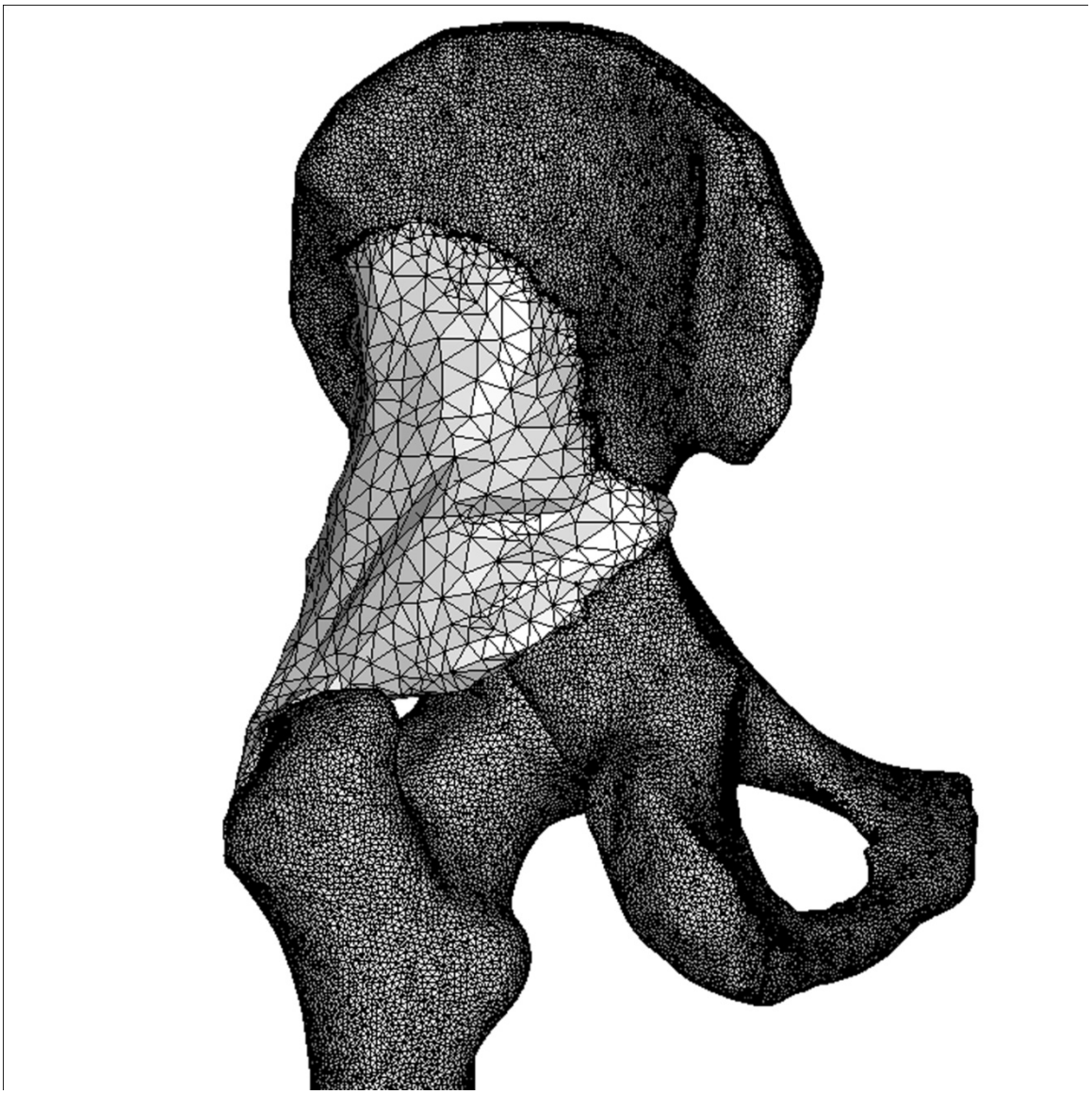

Figure 4.8 Low-resolution gluteus minimus model consisting of 6,995 elements.

CHAPTER 5:

DISCUSSION AND CONCLUSIONS

Discussion

The purpose of this study was to determine if the simplification of a 3-D anatomical model by reducing its number of elements affects the results of FEA. To answer this question, two different phases of analysis were conducted using different representations of the human hip. For Phase 1, the gluteus minimus of each model was decimated in a similar stepwise manner. The model decimation occurred at a rapid rate. The number of elements for the gluteus minimus was decimated to 89% of the original quantity. The plot in Figure 4.3 suggests no overall trend in the relationship between the percentage error of displacement and the percentage of element reduction. The highest error of displacement in a coordinate direction for this model occurred in the Y direction at 0.11% after a 33% reduction in the number of elements. The highest level of error for the total displacement was 0.04% after a 14% reduction. Figure 4.4 reflects the overwhelming consistency of the model. A linear regression t-test was run for each line to determine if the slope was significantly different from 0. With a 99% level of confidence, the null hypothesis (the slope is not equal 0) failed to be

rejected. The remarkably low percentage error of displacement seen in Phase 1 suggests that the model remains very stable despite the dramatic reduction in the number of elements. It should be noted that the solution speed dramatically increased as the complexity of the gluteus minims decreased.

Phase 2 examined the importance of the origin and insertion of the gluteus minimus in the solution of the FEA. When the muscle's origin and insertion were used in conjunction with the representative cylinder, the percentage error in the total displacement was a low 0.10%. The highest percentage of error in the coordinate directions was found in the Y direction with a rate of 0.18%. These results further reflect the stability of the overall model.

The influence of the origin and insertion of the gluteus minimus became evident when they were removed from the model. Without these anatomical structures, the percentage error in the total displacement increased to 2.28%. The highest percentage of error in the coordinate directions was found in the Y direction with a rate of 10.55%. These results suggest that this model's behavior will be relatively constant as long as the origin and insertion of the gluteus minimus remain in intact.

Visually examination of the decimated models reveals that the simplification process contributes to the overall loss in finite and gross anatomical detail. However, the general shape and volume of the gluteus minimus was maintained.

Even at an 89% reduction in the number of elements, the volume of the muscle decreased only 0.25%. This preservation in the models' geometry may have contributed to their overall stability. In the end, the data suggests that 3-D anatomical models can be highly simplified through element reduction without drastically altering the results of FEA as long as the surfaces that receive or apply forces are maintained.

Future Directions

Moving forward with this study, our goal is to increase the level of the model complexity by adding more structures to the hip model to include all the muscles relevant to hip movement as well as a representative joint capsule. It is also the goal to improve the representation of the muscle mechanics. The muscles need to exert the forces on the bones by contracting and relaxing. Future studies should also include the unique biomechanics of tendons. Extending these 3-D geometries into simulations like SIMM or LifeModeler would be of interest. Building from other studies, the level of muscle geometry detail could be examined by taking the individual fiber direction and behavior into account.[38] Another area of interest would be to examine the microstructure and organization of skeletal muscle tissue. From this study, the importance of muscle origin and insertions could be utilized to create a virtual 3-D skeleton that contained the "footprints" of these muscle attachments. Movement arms could then be attached

as needed to the centroid of these attachments to assist in the analysis of movement.

Conclusions

Anatomical geometry plays a critical role in the function of the human body. When analyzing movement, behavior or even designing medical implants, engineers need to account for the 3-D geometry of these structures. The unique shapes and the respective function of anatomical features, such as origins and insertions, add a level of complexity to any potential virtual model. The FEM packages that once only handled the straight lines and standard sets of primitive shapes have been expanded to include more complex objects.

The overall purpose of this study was to examine the effect 3-D model simplification had on FEA of anatomical models. In order to perform a given simulation on an anatomical structure it is often necessary to reduce the overall complexity of the model. The results of this study suggest that anatomical geometries can withstand high levels of simplification without dramatically affecting the results of FEA provided that key anatomical features, such muscle origins and insertions, are preserved. By being aware of the affects of model simplification, biomedical engineers will be able to create anatomical models with the confidence that the results they are capturing accurately reflect the

biomechanics of the system. This will in turn allow for more biomechanical representations for clinical applications.

REFERENCES

(1) Spitzer, V et al. The Visible Human Male: A Technical Report, JAMIA, 1996; 3:118-130.

(2) Audette, MA et al. A procedure for computing patient-specific anatomical models for finite element-based surgical simulation. Internaltional Congress Series, 2003, 1246:356-361.

(3) McCraken, T Ed. New Atlas of Human Anatomy. Barnes & Noble, Inc. 1999.

(4) Schiebinger, L. Skeletons in the closet: The first illustrations of the female skeleton in eighteenth-century anatomy. Representations, 1986, 60:42-82.

(5) Brenner, DJ et al. Estimated radiation risks potentially associated with full-body CT Screening, Radiology, 2004, 243:735-738.

(6) Spitzer, V et al. The Visible Human Male: A Technical Report, JAMIA, 1996; 3:118-130.

(7) Park, JS, et al. Visible Korean Human: its Techniques and Applications. Clinical Anatomy, 2006; 3:216-225.

(8) Zhang, SX, et al. Chinese Visible Human Project. Clinical Anatomy, 2006, 19:204-215.

(9) Clough, Robert. The Finite Element in Plane Stress Analysis. Proc. 2nd ASCE Conf. on Electronic Computation. Pittsburgh, Pa., Sept. 1960.

(10) Zienkiewicz, O. and R. Taylor. The Finite Element Method Volume 1: The Basis. Oxford: Butterworth-Heinemann, 2000.

(11) Liu, G. and S. Quek. The Finite Element Method A Practical Course. Oxford: Butterworth-Heinemann, 2003.

(12) Dumont, E. Biomesh. FEA in Biology. June 12, 2010. http://www.biomesh.org.

(13) Bayraktar, HH et al. Comparison of the elastic and yield properties of human and cortical bone tissue. Journal of Biomechanics, 2004, 37:27-35.

(14) Hofmann, T et al. Assessment of composition and anisotropic elastic properties of secondary osteon lamellae. Journal of Biomechanics, 2006, 39:2282-2294.

(15) Kaneko, TS et al. Mechanical properties density and quantitative CT scan data of trabecular bone with and without metastases. Journal of Biomechanics, 2004, 37:523-530.

(16) Staubli, HU, et al. Mechanical tensile properties of the quadriceps tendon and patellar ligament in young adults. The American Journal of Sports Medicine, 1999, 27:27-34.

(17) Rotter, N. et al. Age-related changes in the composition and mechanical properties of human nasal cartilage. Archives of Biochemistry and Biophysics, 2002, 403:132-140.

(18) Combs, SA and TL Danial. Into Thin Air: Contributions of Aerodynamic and Intertial-Elastic Forces to Wing Benging in the Hawkmoth Manduca sexta. Journal of Experimental Biology.2003, 206:2999-3006.

(19) McHenry, CR. et al. Biomechanics of the Rostrum in Crocodilians: a Comparitive Analysis using Finite-Element Modeling. The Anatomical Record: Advances in Integrative Anatomy and Evolutionary Biology. 2006, 288:827-849.

(20) Dumont, E. et al. Finite-Element Analysis of Biting Behavior and Bone Stress in the Facial Skeletons of Bats. The Anatomical Record, 2005, 283:319-330.

(21) Arbour, VM, and E Snively. Finite Element Analyses of Anklosaurid Dinosaur Tail Club Impacts. The Anatomical Record: Advances in Intergrative Anatomy and Evolutionary Biology. 2009, 292(9):1412-1426.

(22) Fourcauld, T. and P Lac. Numerical Modelling of Shape Regulation and Growth Stresses in Trees I: An Incremental Static Finite Element Formulation. Trees 2003, 19:23-30.

(23) Dumont, E. et al. Requirements for Comparing the Performance of Finite Element Models of Biological Structures. Journal of Theoretical Biology, 2009, 256:96-103.

(24) Brekelmans, WA, et al. A New Method to Analyse the Mechanical Behavior of Skeletal Parts. Acta Orthopaedica, 1972, 43(5):301-317.

(25) Arab-Ghanbari, M. et al. Analysis of Blood Turbulent Flow in Carotid Artery Including the Effects of Mural Thrombosis Using Finite Element Modeling. American Journal of Applied Sciences. 2009, 6(1):337-345.

(26) Khani, M. et al. Dynamic Stress Analysis of the Arterial Wall Utilizing Physiological Pressure Waveforms. American Journal of Applied Sciences. 2008, 5:1285-1291.

(27) Gu, YD. et al. Computer Simulation of Stress Distribution in the Metatarsals as Different Inversion Landing Angles Using the Finite Element Method. International Orthopaedics. 2010, 34(5):669-676

(28) Cilingir, AC. et al. Three-Dimensional Anatomic Finite Element Modeling of Hemi-Arthroplasty of Human Hip Joint. Trends in Biomaterials & Artificial Organs. 2007, 21(1):63-72.

(29) Zhai, J. and G. Narwani. Development of a Human Body Finite Element Model for Restraint System R&D Applications. Proceedings 19th International Technical Conference on the Enhanced Safety of Vehicles. 2005. Washington DC.

(30) Helwig, P. et al. Finite Element Analysis of a Bone-Implant System with the Proximal Femur Nail. Technology and Healthcare, 2006, 14:411-419.

(31) Delp, SL et al. Transfer of the rectus femoris: Effects of transfer site on moment arms about the knee and hip. Journal of Biomechanics, 1995, 13(1):96-104.

(32) Hoy, MG et al. A musculoskeletal model of the human lower extremity: The effect of muscle, tendon, and moment arm on the moment-angle relationship of musculotendon actuators at the hip, knee and ankle. Journal of Biomechanics, 1990, 23(2):157-169.

(33) Chai, E et al. Simulation and animation of musculoskeletal joint system. Journal of Biomechanical Engineering. 1993, 115:562-568.

(34) Musculographics Inc. SIMM. August 10, 2010. http://musculographics.com/products/simm.html

(35) LifeModeler. August 10, 2010. https://www.lifemodeler.com/

(36) Delp, SL et al. A Computational framework for simulating and analyzing human and animal movement. IEEE Computing in Science and Engineering. 2000, 2(5):46-55.

(37) Rehorn, MR et al. The effects of aponeurosis geometry on strain injury susceptibility expored with a 3D muscle model. Journal of Biomechanics, 2010, 43:2574-2581.

(38) Blemker, SS et al. Three-Dimensional Representation of Complex Muscle Architectures and Geometries. Annals of Biomedical Engineering, 2005, 33(5):661-673.

(39) Beck, M. et al. The anatomy and function of the gluteus minimus muscle. Journal of Bone and Joint Surgery, 2000, 82:358-363.

(40) Drake, R. et al. Gray's Anatomy for Students. Elsevier Inc. Canada. 2005.

(41) Pugh, M et al. Stedman's Medical Dictionary. 27th Ed. Lippincott Williams & Wilkins. Baltimore, MD. 2000.

(42) United States National Library of Medicine. The Visible Human Project. September 18, 2010. http://www.nlm.nih.gov/research/visible/visible_human.html.

(43) Bangash, MYH et al. Trama – An Engineering Analysis: With Medical Case Studies Investigation. Springer. New York, 2007.

(44) Muller, SS et al. Comparative analysis of the mechanical properties of the patellar ligament and calcaneus tendon. Acta Ortopedica Brasileira, 2004, 12(3):134-140.

ABOUT THE AUTHOR

Jonathan M. Ford was born in Las Vegas, Nevada and earned a dual baccalaureate with honors in English and History from the University of Nevada Las Vegas. In 2009, he earned his Master's of Science in Medical Science (Anatomy) from the University of South Florida (USF) College of Medicine. Since 2008 he has been a graduate research assistant at the Center for Human Morpho-Informatics Research in the USF College of Medicine. While working for Dr. Don Hilbelink, he has served as a teaching assistant and biomedical engineering researcher. Currently he is working on his Ph.D. in Biomedical Engineering at the USF College of Engineering.